Yang Xuan, Shian Jia and Laurentiu Nastac*

Processing and Microstructure Characteristics of As-Cast A356 Alloys Manufactured via Ultrasonic Cavitation during Solidification

DOI 10.1515/htmp-2016-0147
Received July 5, 2016; accepted December 23, 2016

Abstract: Recent studies have showed that the microstructure and mechanical properties of A356 alloy can be significantly improved when ultrasonic cavitation and solidification processing is used. This is because during the fabrication of A356 castings, ultrasonic cavitation processing plays an important role in degassing and refining the as-cast microstructure. In the present study, A356 alloy and Al_2O_3/SiC nanoparticles are used as the matrix alloy and the reinforcements, respectively. Nanoparticles are injected into the molten alloy and dispersed by ultrasonic cavitation. Ultrasonic cavitation was also applied during solidification of these nanocomposites. The microstructure and nanoparticle distribution of the cast samples have been investigated in detail. The current experimental results indicated that ultrasonic cavitation during solidification will greatly improve the microstructure of the samples. Al_2O_3 and SiC nanoparticle reinforced nanocomposites have different nanoparticle distributions in the matrix.

Keywords: ultrasonic cavitation, A356 alloy, nanocomposites, microstructure, nanoparticle dispersion

PACS® (2010). 81.05

Introduction

Aluminum matrix composites are attractive for application in automobile, aerospace industries because of their desirable properties, such as low density, high specific strength, high wear resistance, high specific stiffness, low price and so on [1–9]. It has been proved that microstructure and mechanical properties of a casting product can be significantly improved if use nano-sized ceramic particles as reinforcement to fabricate metal-matrix-nanocomposites (MMNCs). There are several fabrication methods of MMNCs, like Ultrasonic Stirring Technology (UST), sol-gel synthesis, laser deposition, high energy milling, ball milling, etc. The key part of fabricate MMNCs is the mixing of nano-sized ceramic particles [10–13].

There are different types of nanoparticles that can be used as reinforcement to fabricate Al-based MMNCs, such as Al_2O_3, β-SiC, ZrC, TiN, etc. Jia et al. [14, 15] have determined that the optimum type of nanoparticles was Al_2O_3 or SiC because of their relatively good chemical and thermal stability. They also determined that the optimum amount of those nanoparticles are 1.0 mass%. Some experimental work and simulation results [16–18] have shown that UST is a promising way to fabricate MMNCs. Since UST will induce nonlinear effects like cavitation and acoustic streaming into the melt, it will be very helpful to spread and break the de-agglomeration of nanoparticles in the matrix.

If UST treatment is used during the solidification process, it will induce pressure and temperature oscillations in the melt, which will help increase heterogeneous nucleation and enhance dendrite fragmentation. Recently work indicates that UST during solidification can effectively refine grain structure for Mg-Al based alloys, ice generation, etc. [19–21]. However, there is not significant amount of research regarding UST treatment during solidification for Al-based MMNCs.

Experimental approach

In this study, aluminum alloy A356 is used as the metallic matrix. There are two different nanoparticles been used: Al_2O_3 (spherical shape, average diameter is about 20 nm) and β-SiC (spherical shape, average diameter is 45–55 nm). An induction furnace was used to melt A356 alloy. Sketch of the ultrasonic processing system is shown in Figure 1. Ultrasonic equipment parameters are shown following: maximum power is 2.4 kW; frequency is 18 kHz, the diameter of the Nb ultrasonic probe is 40 mm and the probe amplitude is around 20 μm.

Five different types of cast samples have been fabricated in this study. The control group experiment is done

***Corresponding author: Laurentiu Nastac,** The University of Alabama, Tuscaloosa, AL 35487, USA, E-mail: lnastac@eng.ua.edu
http://orcid.org/0000-0002-8979-0680
Yang Xuan, Shian Jia, The University of Alabama, Tuscaloosa, AL 35487, USA

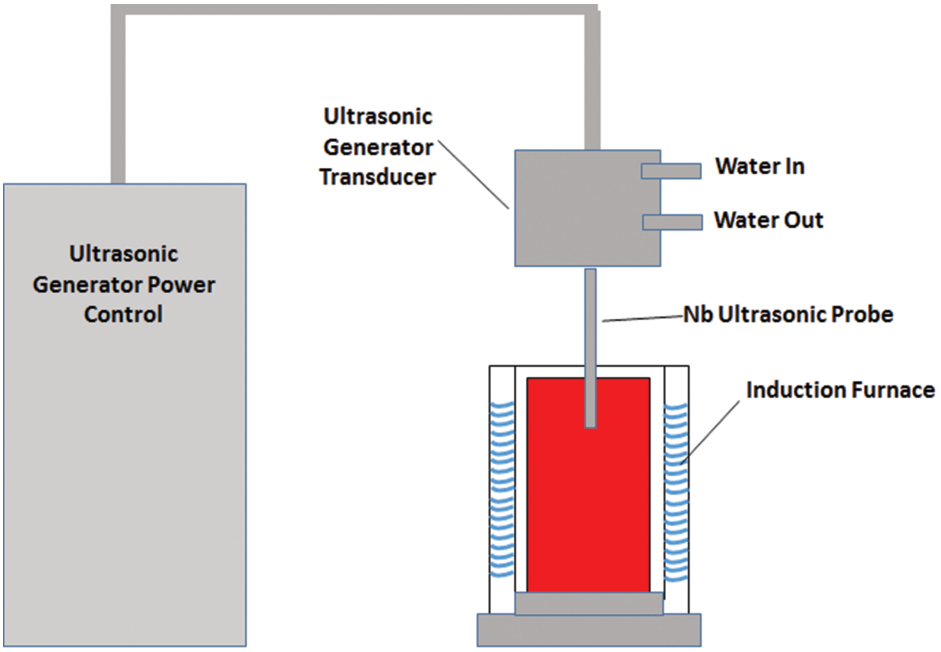

Figure 1: A schematic representation of the UST and induction furnace equipment.

by melting the A356 alloy in furnace, when melt temperature reach 750 °C, turn off the furnace to let the molten metal solidify in the furnace. The UST experiment is done by melting the A356 alloy and turn off the furnace when melt temperature reach 750 °C, treating the molten alloy with UST during solidification for about 3 min and then let the melt solidify in the furnace. The UST experiments with nanoparticles (Al_2O_3 or SiC are done by melting the A356 alloy; when temperature reaches 750 °C, 1.0 mass% nanoparticles (Al_2O_3 or SiC) assisted by UST were added for about 15 min keeping the melt temperature at 750 °C, then turn off the furnace; use UST treatment during furnace solidification for 3 min then let the melt solidify in the furnace. The fifth sample was obtained as follows: an A356 alloy with 1.0 mass% Al_2O_3 nanoparticles was treated by UST for about 15 min after the melt temperature reached 750 °C; then the furnace was turned off to let the molten metal solidify inside the furnace.

The Nb ultrasonic probe was inserted to about 25 mm beneath the melt surface to perform the UST treatment during solidification.

Results and discussion

The cast ingots are cylindrical in shape, the ingot diameter is 65 mm and its height is 70 mm. The ingots have been split into half, then cut the halves into three parts and labeled as top, middle and bottom, as shown in Figure 2.

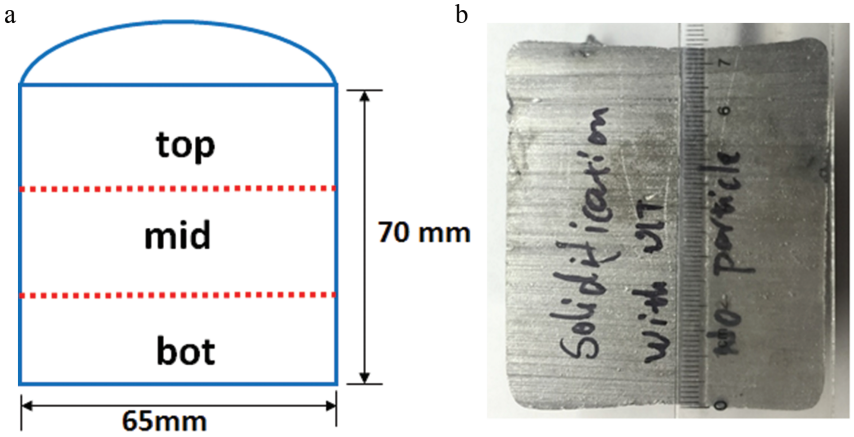

Figure 2: (a) Representation of cast ingots. (b) Representation of cast ingots.

The microstructures of the middle and bottom parts

Figure 3 shows the optical microscopy results in the middle part of the cast ingots. As shown in Figure 3(a) and (b), the A356 samples without UST treatment during solidification have coarser microstructures than the ones with UST treatment. Applying UST during solidification can break up the dendritic structure and thus more fine globular grain structure can be obtained. Figure 3(c) and (d) shows the microstructure of A356 with nanoparticles (Al_2O_3 or SiC) with UST treatment during solidification. They have similar microstructures with those shown in Figure 3(b), which means adding nanoparticles will not change the microstructure significantly, and the UST is the main cause of grain refinement. This is confirmed by Figure 3(e), which shows that coarser dendritic grains were obtained in the middle part of the A356 sample reinforced with 1.0 mass% Al_2O_3 processed without UST treatment during solidification.

The mechanisms of how UST during solidification refine the microstructure can be related to the pressure and temperature cycle change in the melt. They are probably enhancing dendrite fragmentation and increase heterogeneous nucleation in the melt during solidification [22]. UST can produce strong convection and shock waves. Strong convection can cause and promotes diffusion of solute, what's more, convection will cause local temperature and composition variations. Shock waves can induce the breakage of the melting root. Since dendrites usually start melting at

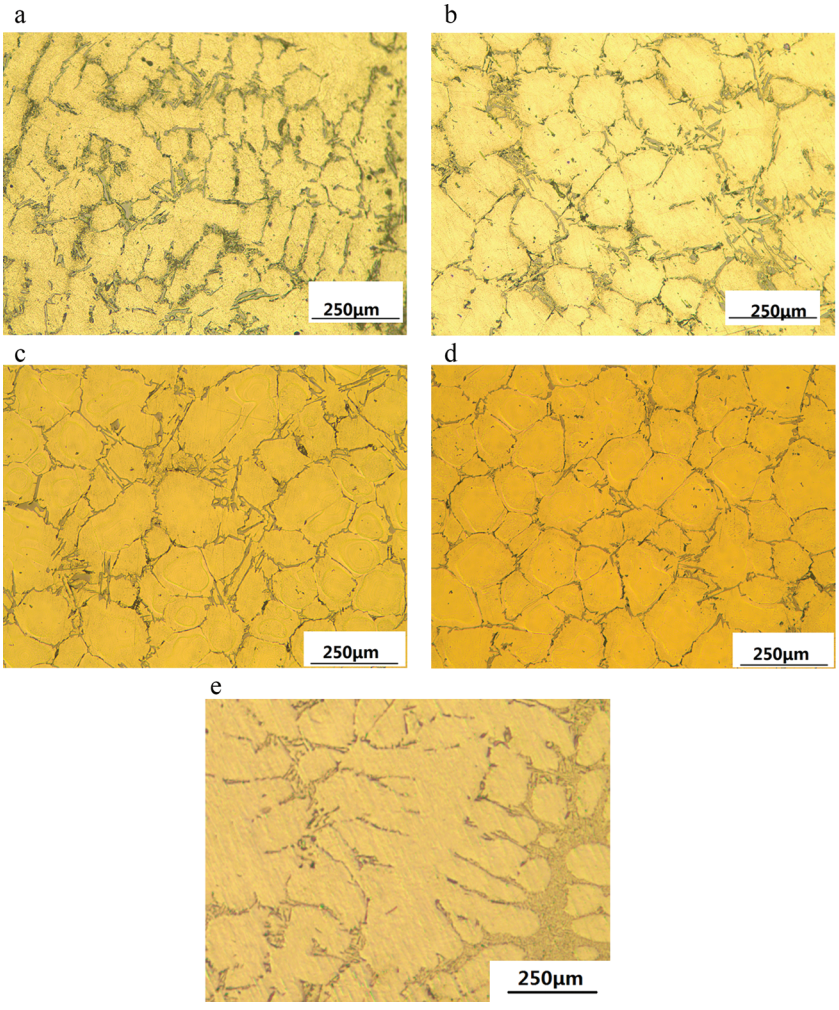

Figure 3: Optical micrographs in the middle part of the cast samples (a) A356 without UST treatment [9] and (b) A356 with UST treatment during solidification and (c) A356 sample reinforced with 1.0 mass% Al_2O_3 and UST during solidification and (d) A356 sample reinforced with 1.0 mass% SiC and UST during solidification and (e) A356 sample reinforced with 1.0 mass% Al_2O_3 without UST during solidification.

the root because of local temperature rise and segregation, UST can promote dendrite fragmentation. On the other hand, when applying UST, melt temperature will change periodically at high frequencies, which means some part of melt is superheated and some part is undercooled. This phenomenon causes increase of nuclei in the melt, which will refine the microstructure [23].

The microstructure of the top part

The height of the top part of the ingots is about 25 mm, which is the part that is adjacent to the ultrasonic probe. As shown in Figure 4(a), the microstructure of A356 obtained via 3 min UST treatment during solidification is dendritic grain, which fits the conclusion of some literature very well [24]. In [24], the authors indicated that the ultrasonic grain refinement occurs almost below the radiating face of the probe, so microstructure of the top part is not as good as the part below the radiating face of the probe. However, all the top part of the samples with the added nanoparticles (Al_2O_3 or SiC) and UST during solidification have fine globular grains, as shown in Figure 4(b) and (c). However, the microstructure of the top part of the A356 sample reinforced with 1.0 mass% Al_2O_3 without UST during solidification consists of dendritic grains, which is similar with the microstructure shown in Figure 4(a). Figure 4 indicates that the microstructure of the ingot section adjacent to the immersed cylindrical face of the probe can be modified only if both the "addition of nanoparticles" and the "use of UST during solidification" approaches are considered. Applying UST during solidification or adding nanoparticles alone will not change the morphology of the top part microstructure from a dendritic grain to a globular grain. The reason for this can be explained as follows: when applying UST during solidification, the ultrasound intensity of the top part is so weak that it cannot increase the nucleation potential or enhance the dendrite fragmentation (as shown in Figure 4(a)). The added nanoparticles are disperse very well into the melt, but nanoparticles have no effect on grain refinement (as shown in Figure 4(d)) until UST is applied during solidification. The nanoparticles (Al_2O_3 or SiC) in the top part will be activated by weak ultrasound, which in turn will increase the nucleation potential during solidification, and consequently to refine the microstructure (as shown in Figure 4(b) and (c)). In addition, since the ultrasound intensity in the middle and bottom parts is strong enough to refine the microstructure (increase nucleation and enhance dendrite fragmentation), the effect

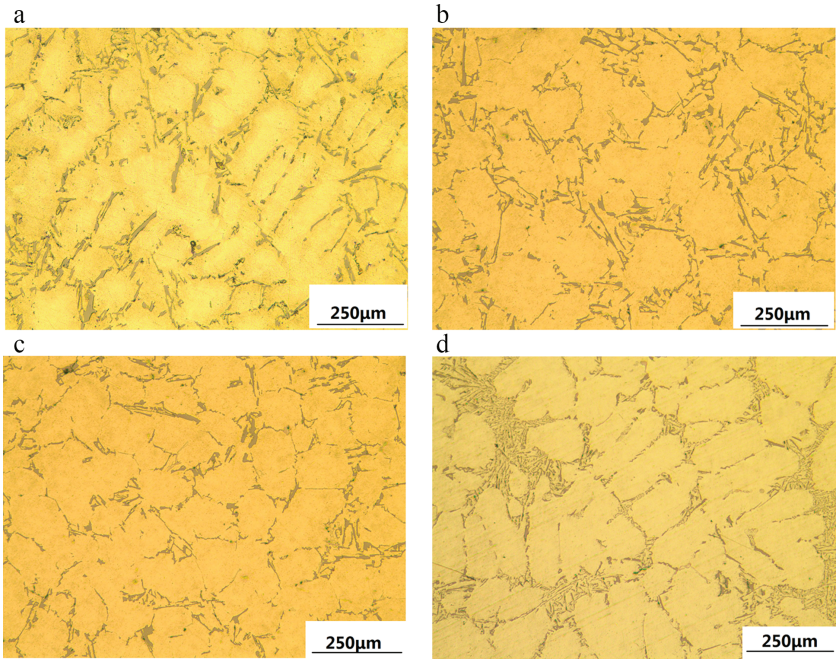

Figure 4: Optical micrographs for the top part of the cast samples (a) A356 with UST treatment during solidification and (b) A356 sample reinforced with 1.0 mass% Al_2O_3 and UST during solidification and (c) A356 sample reinforced with 1.0 mass% SiC and UST during solidification and (d) A356 sample reinforced with 1.0 mass% Al_2O_3 without UST during solidification.

of the UST activated nanoparticles on the microstructure refinement cannot be distinguished.

Globular grain size distribution

Table 1 shows the globular grain size distribution of the measured samples at various locations. The microstructures of the control group and of the top location of the A356 samples obtained via 3 min UST during solidification have not been measured because they are not revealing pure globular grain structures.

Table 1: Globular grain size distribution of the measured samples at various locations.

	UST	1.0 mass% Al_2O_3 + UST	1.0 mass% SiC + UST
Top	/	119 ± 14.6μm	120 ± 11.0μm
Middle	126 ± 12.7μm	142 ± 10.7μm	132 ± 11.3μm
Bottom	151 ± 12.9μm	173 ± 9.6μm	179 ± 11.4μm

Table 1 shows that for each ingot, the grain size increases from top to bottom and top location has the smallest grain size. The bottom-location globular grain size of A356 samples obtained via 3 min UST during solidification is 151 μm, which is 19.8 % larger than that in the middle location. The addition of the Al_2O_3 nanoparticles can refine the top-location microstructure, grain size of the ingot in the middle location is 19.3 % larger than that in the top location; the bottom-location globular grain size is 45.3 % larger than that in the top location and 21.8 % larger than that in the middle location. The addition of the SiC nanoparticles can refine the microstructure in the top location, grain size of the ingot in the middle location is 10.0 % larger than that in the top location. The globular grain size in the bottom region is 49.0 % larger than that in the top location and 35.6 % larger than that in the middle location. Higher the UST intensity, smaller the grain size; basically the grain size differences indicate the UST intensity differences [24]. The results in Table 1 indicate that UST intensity in the current experiment is high enough to refine the entire ingot microstructure and UST intensity decreases with increasing distance from the radiating face. The globular grain size in top part is smaller than that in the middle and bottom parts of the samples with the added nanoparticles (Al_2O_3 or SiC) and UST during solidification because of the faster cooling rates from the top of the furnace, which was exposed to air cooling, and because of its contact with the ultrasonic probe, which was water cooled.

When compare the same location of different samples, A356 samples without nanoparticles have the smallest grain size. Regarding the globular grain size in the middle location, the addition of the Al_2O_3 nanoparticles increases the grain size by 12.7 % when comparing with that without nanoparticles; the addition of the SiC nanoparticles increases the grain size by 4.7 % when comparing with that without nanoparticles. Regarding the globular grain size in the bottom location, the increase is 14.6 % and 18.5 %, respectively. The comparison results indicate that by adding the nanoparticles the globular grain size will further increase.

Nanoparticle distribution

Figure 5 shows the SEM microstructures at high magnification of the A356 sample reinforced with 1.0 mass % Al_2O_3 and UST during solidification. Many nanoparticles can be found in the matrix as highlighted by the red circle in Figure 5(b) and (c). Those nanoparticles have spherical shape and average size of about 20 nm, which are similar in size with the nanoparticles added during the processed ingots. The SEM results indicate that the Al_2O_3 nanoparticles are dispersed reasonably well into the A356 matrix.

Figure 6(a) and (b) shows the SEM microstructures at high magnification of the A356 sample reinforced with 1.0 mass % SiC and UST during solidification. Unlike the results in the A356 sample obtained by adding Al_2O_3, a significant number of nanoparticles in Figure 6(b) has been found in the grain boundary area. Those nanoparticles have spherical shape and average size is less than 50 nm, which is similar in size with the nanoparticles added during the manufacturing process. Since the particles are in nanometer size, the EDS accuracy is not enough to identify the particle chemical composition, therefore Figure 6(c) only shows the EDS mapping results at relatively low magnification. In the mapping photo, the red color represents C (carbon), the green color represents Al (aluminum). The EDS results indicated that some of C tends to stay in the grain boundary area. By combining the EDS results with the SEM photo, it can be estimated that the SiC nanoparticles are mostly gather around the grain boundary area.

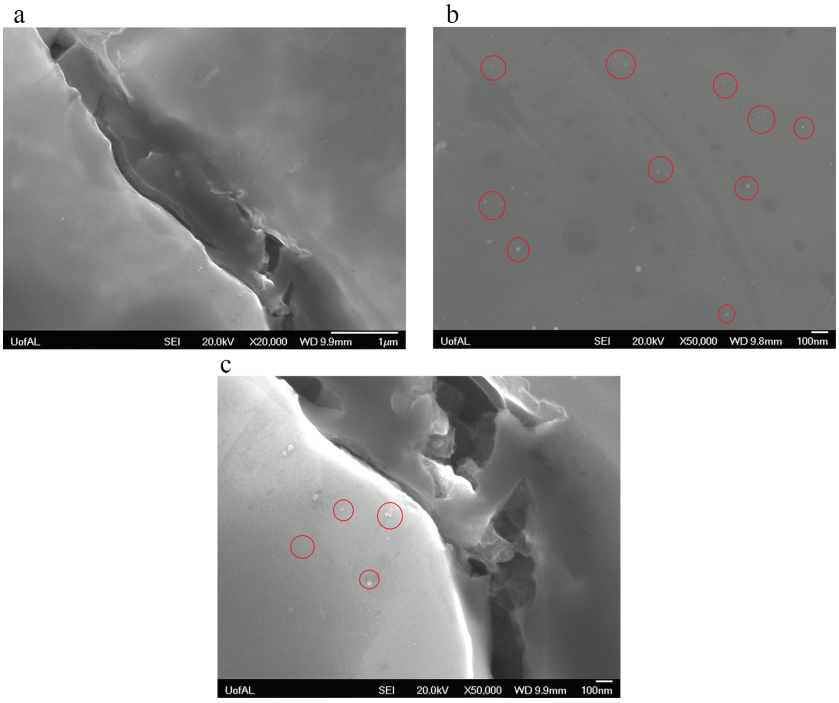

Figure 5: SEM results of the sample processed with UST + 1.0 mass% Al_2O_3, the red circles highlight the location of the nanoparticles. (a) at X20000 and (b) at X50000 and (c) at X50000.

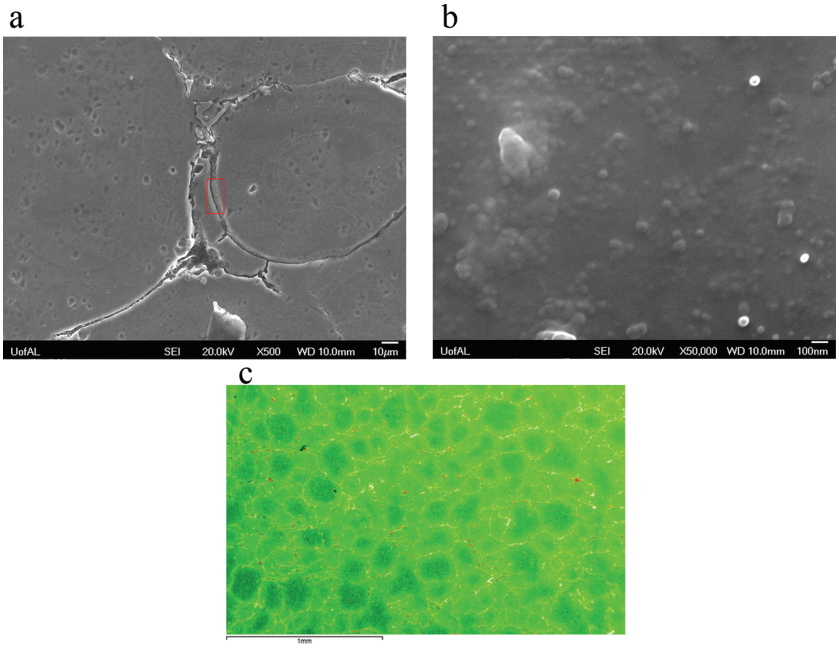

Figure 6: SEM results and EDS mapping photo of the sample processed via UST + 1.0 mass% SiC. (a) SEM picture at X500 and (b) SEM picture of red rectangular area in (a) at X50000 and (c) EDS mapping results at X40.

Conclusions

This study determined that the UST treatment during solidification plays a key role in refining the microstructure of the A356 cast ingots. Without UST processing, dendritic structure was obtained; by using UST during solidification, fine globular grain structure was obtained. The addition of the nanoparticles (Al_2O_3 or SiC) is not the main cause for microstructure refinement, however, when UST is applied during solidification, the nanoparticles can modify the

microstructure of the ingot part adjacent to the immersed cylindrical face of the probe.

It was determined that the globular grain size increases with increasing the distance from the radiating face. The addition of the nanoparticles (Al_2O_3 or SiC) will slightly increase the grain size.

The SEM and EDS results indicated that the added Al_2O_3 nanoparticles are dispersed reasonably well into the A356 matrix. Some added SiC nanoparticles into the A356 matrix are gathered around the grain boundary area.

Acknowledgments: Authors wish to express thanks to the China Scholarship Council (CSC) for the financial support.

References

[1] B. Su, H.G. Yan, G. Chen, J.L. Shi, J.H. Chen and P.L. Zeng, Mater. Sci. Eng. A, 527 (2010) 6660–6665.
[2] S.M. Seyed Reihani, Mater. Des., 27 (2006) 216–222.
[3] D. Bozic, B. Dimcic, O. Dimcic, J. Stasic and V. Rajkovic, Mater. Des., 31 (2010) 134–141.
[4] M.P. De Cicco, X. Li and L.-S. Turng, J. Mater. Proc. Technol., 209 (2009) 5881–5885.
[5] C.S. Goh, J. Wei, L.C. Lee and M. Gupta, Mater. Sci. Eng. A, 423 (2006) 153–156.
[6] A.B. Elshalakany, T.A. Osman, A. Khattab, B. Azzam and M. Zaki, J. Nanomater., 2014 (2014) 1–14.
[7] X. Liu, S. Jia and L. Nastac, Int. J. Met. Cast (AFS), 8(3) (2014) 51–58.
[8] S. Jia, P.G. Allison, T.W. Rushing and L. Nastac, Advances in the science and engineering of casting solidification: an MPMD symposium honoring Doru Michael Stefanescu John Wiley & Sons, Inc. (2015), pp. 31–36.
[9] S. Jia, D. Zhang, Y. Xuan and L. Nastac, Appl. Acoust., 103 (2016) 226–231.
[10] K. Akio, O. Atsushi, K. Toshiro and T. Hiroyuki, J. Jpn. Inst. Light Met., 49(4) (1999) 149–154.
[11] X.F. Chen, E.G. Baburai, F.H. Froes and A. Vassel, Advanced Particulate Materials and Processes International Conference, April 7–9, 1997, West Palm Beach, Florida (1997), pp. 185–192.
[12] S.L.U. Filho, R. Rodriguez, J.C. Earthman and E.J. Lavernia, Mater. Sci. Forum, 416–418 (2003) 213–218.
[13] J.R. Groza, Int. J. Powder Metall., 35 (1999) 59–66.
[14] S. Jia, X. Liu and L. Nastac, Proceedings of the Advanced Casting Technologies Symposium, TMS, March 11–15, 2012, Orlando, Florida (2012), pp. 112–119.
[15] S. Jia and L. Nastac, Chem. Mater. Eng.1 , (2013) 69–73.
[16] D. Zhang and L. Nastac, J. Mater. Res. Technol., 3(4) (2014) 296–302.
[17] D. Zhang, S. Jia, P. Allison and L. Nastac, Proceedings of the "Advanced metal casting technologies" symposium, TMS, October 12–16, 2014, Pittsburgh, PA (2014), pp. 695–702.
[18] S. Jia, D. Zhang and L. Nastac, J. Mater. Eng. Perform., 24(6) (2015) 2225–2233.
[19] G.I. Eskin and D.G. Eskin, Ultrasonic Treatment of Light Alloy Melts, second edition, CRC Press (2014).
[20] Z. Xu, J. Yan, W. Chen and S. Yang, Mater. Lett., 62 (2008) 2615–2618.
[21] X. Zhang, T. Inada, A. Yabe, S. Lu and Y. Kozawa, Int. J. Heat Mass Transfer, 44 (2001) 4533–4539.
[22] X. Jian, H. Xu, T.T. Meek and Q. Han, Mater. Lett., 59(2–3) (2005) 190–193.
[23] D.M. Herlach, K. Eckler, A. Karma and M. Schwarz, Mater. Sci. Eng. A, 304–306 (2001) 20–25.
[24] M. Qian and A. Ramirez, Chapter 8 in Ultrasonic Grain Refinement of Magnesium and Its Alloys, Magnesium Alloys – Design, Processing and Properties edited by Frank Czerwinski InTech ,(2011), pp. 163–186.